Supplemental Figure 1 (related to Figure 1): Competitive transplantations at 1:100 dilution into wildtype (*WT*) recipients with *WT* competitor cells

A Competitive transplantations at 1:100 dilution into wildtype (*WT*) recipients with *WT* competitor cells

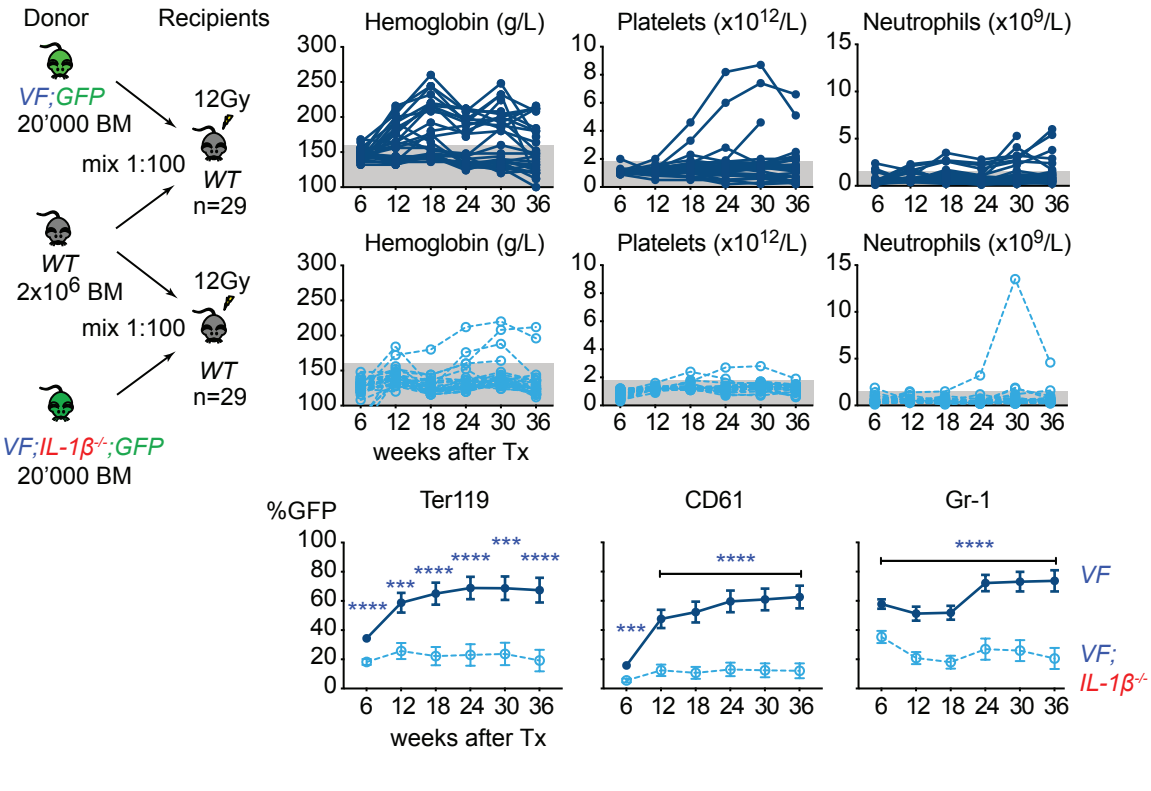

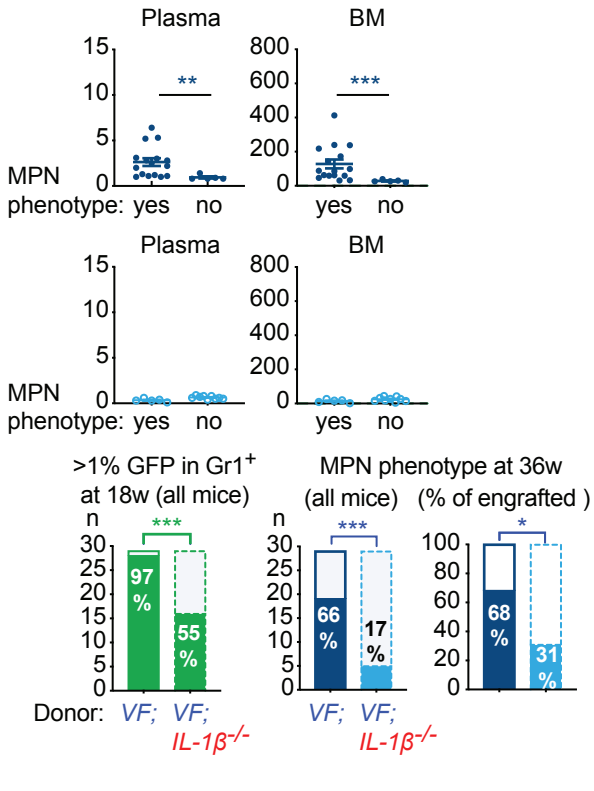

B Complete blood count and GFP chimerism in mice that developed MPN phenotype (with *WT* competitor cells)

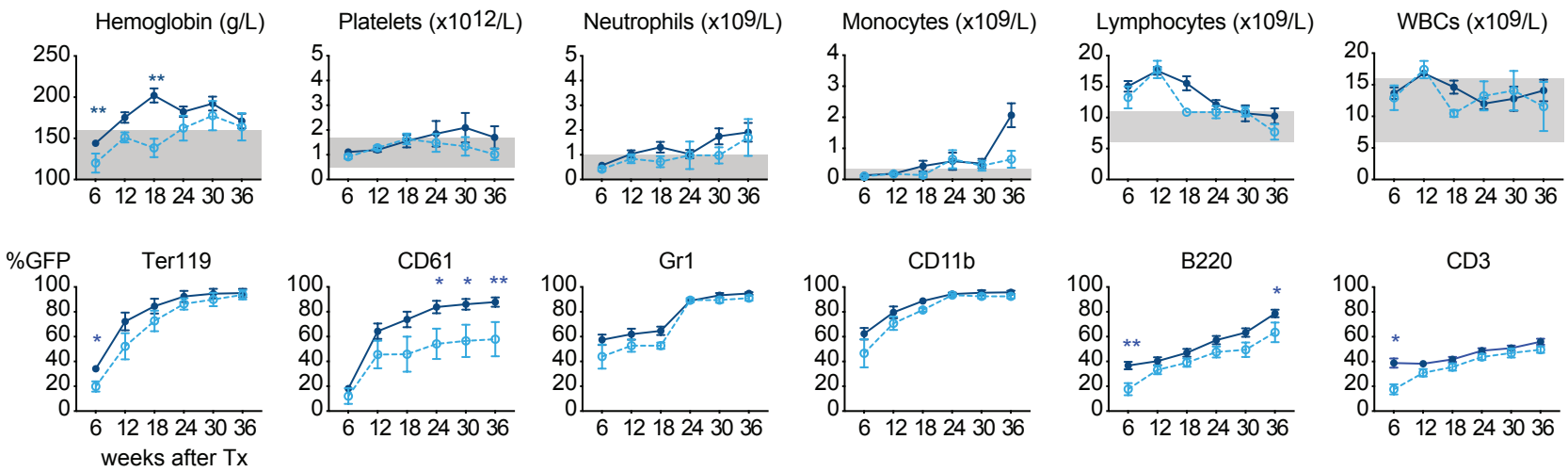

C GFP-Chimerism in HSPCs of mice that developed MPN phenotype at 36w

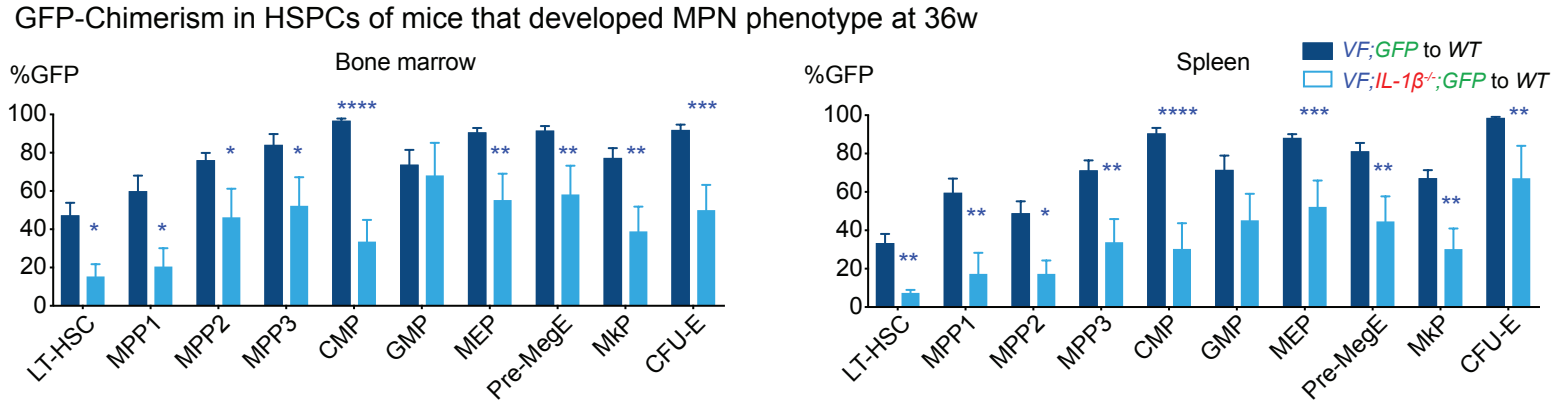

D Reticulin fibrosis in mice that developed MPN phenotype at 36w

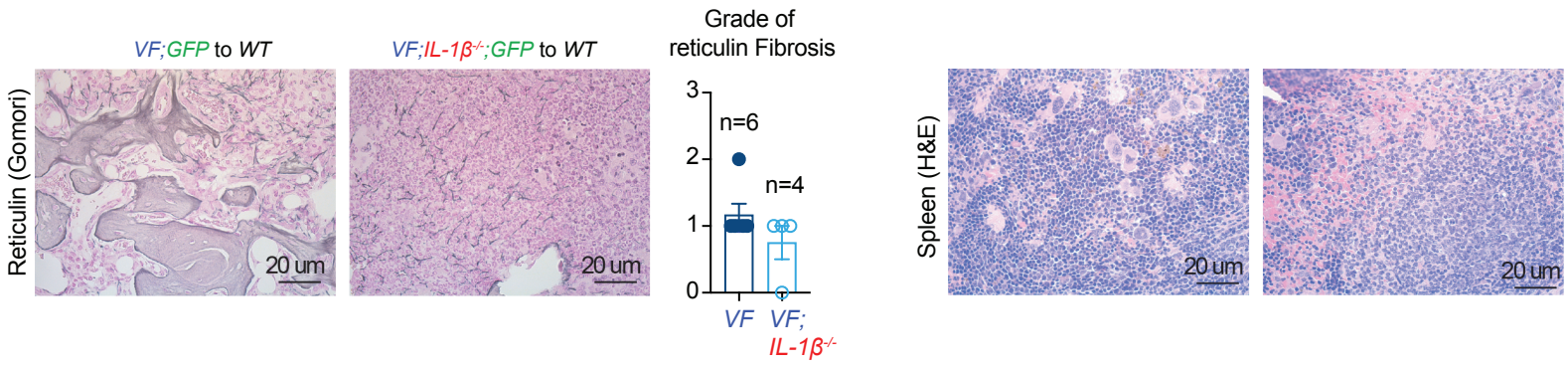

E Inflammatory cytokines in BM and Plasma of mice that developed MPN phenotype at 36w

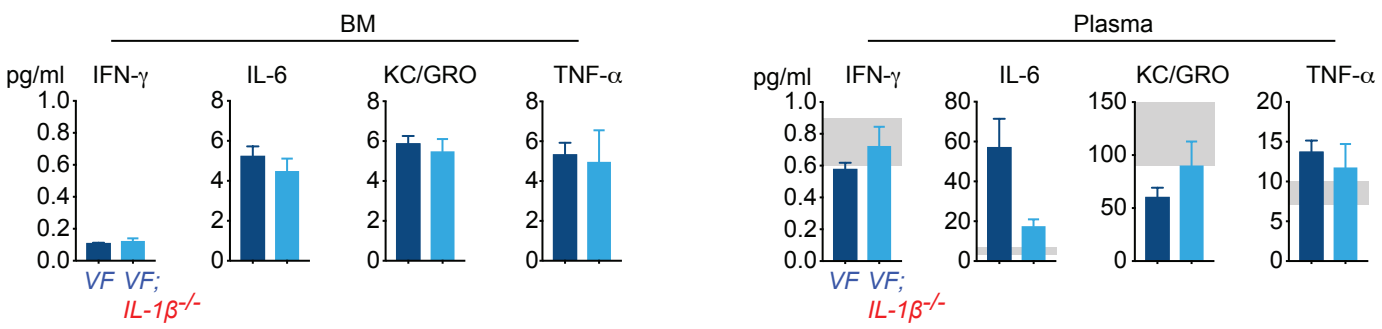

Legend to Supplemental Figure 1 (related to Figure 1)

Supplemental Figure 1. Loss of *IL-1β* from *JAK2*-mutant hematopoietic cells reduces MPN disease initiation (Transplantation at 1:100 dilution into *WT* recipients with BM competitor cells from a *WT* donor). (A) Schematic drawing of the experimental setup for competitive transplantation at 1:100 dilution. Bone marrow (BM) from *VF;GFP* or *VF;IL-1β-/-;GFP* donor mice was mixed with a 100-fold excess of BM competitor cells from a *WT* donor. The time course of blood counts from individual mice that received BM from *VF;GFP* (upper panel) or *VF;IL-1β-/-;GFP* donors (middle panel), and the GFP chimerism in peripheral blood (lower panel) are shown. Multiple t tests were performed for statistical analyses. IL-1β protein levels in plasma and BM lavage (1 femur and 1 tibia) of mice with or without MPN phenotype is shown (right panel). Non-parametric Mann-Whitney two-tailed t test was performed for statistical comparisons. Bar graphs (bottom right) show the percentages of mice that showed engraftment defined as GFP-chimerism >1% at 18 weeks after transplantation and the percentages of mice that developed MPN phenotype (elevated hemoglobin and/or platelet counts). p values in lower panel were computed using Fisher's exact test. **(B)** Time course of mean blood counts and GFP chimerism in peripheral blood of *WT* mice transplanted with BM from *VF;GFP* or *VF;IL-1β-/-;GFP* and *WT* competitor cells that developed MPN phenotype during 36-weeks follow-up. Multiple t tests were performed for statistical analyses. **(C)** GFP-chimerism in hematopoietic stem and progenitor cells (HSPCs) at 36 weeks after transplantation in BM (left) and spleen (right) of *WT* mice transplanted with BM from *VF;GFP* or *VF;IL-1β-/-;GFP* and *WT* competitor cells that developed MPN phenotype. Multiple t tests were performed for statistical analyses. **(D)** Representative images of reticulin fibrosis staining in BM (left panel) and H&E staining in spleen (right panel) of mice showed MPN phenotype at 36 weeks after transplantation. Histological grade of reticulin fibrosis in BM is shown in a bar graph (right). **(E)** Levels of Inflammatory cytokines in BM lavage (1femur and 1 tibia) and plasma of mice that displayed MPN phenotype at 36 weeks after transplantation. Grey shaded area represents normal range. All data are presented as mean ± SEM. *P < .05; **P < .01; ***P < .001; ****P < .0001.

Supplemental Figure 2 (related to Figure 1)

A Competitive transplantations at 1:100 dilution into *IL-1β*$^{-/-}$ recipients

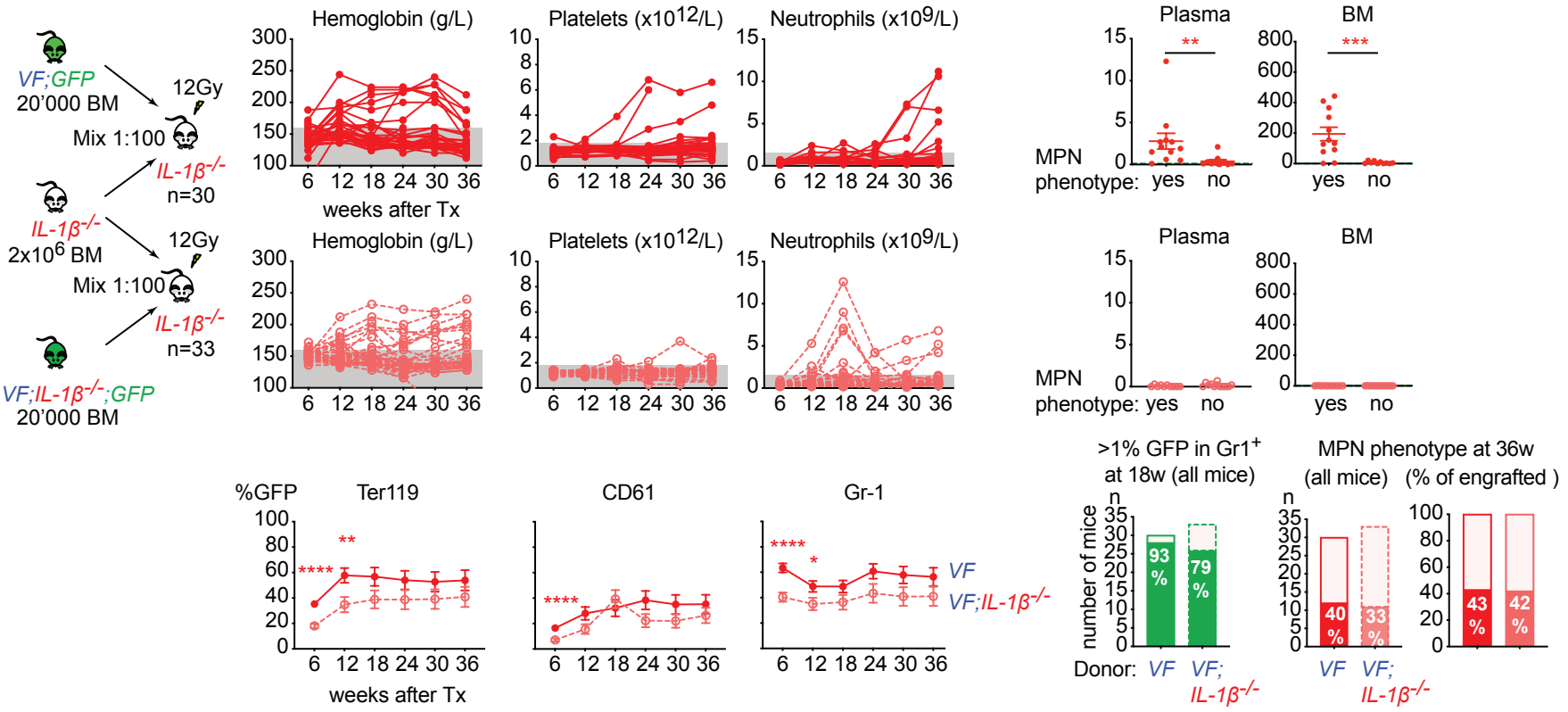

B Complete blood count and GFP chimerism in *IL-1β*$^{-/-}$ recipient mice that developed MPN phenotype at 36 weeks

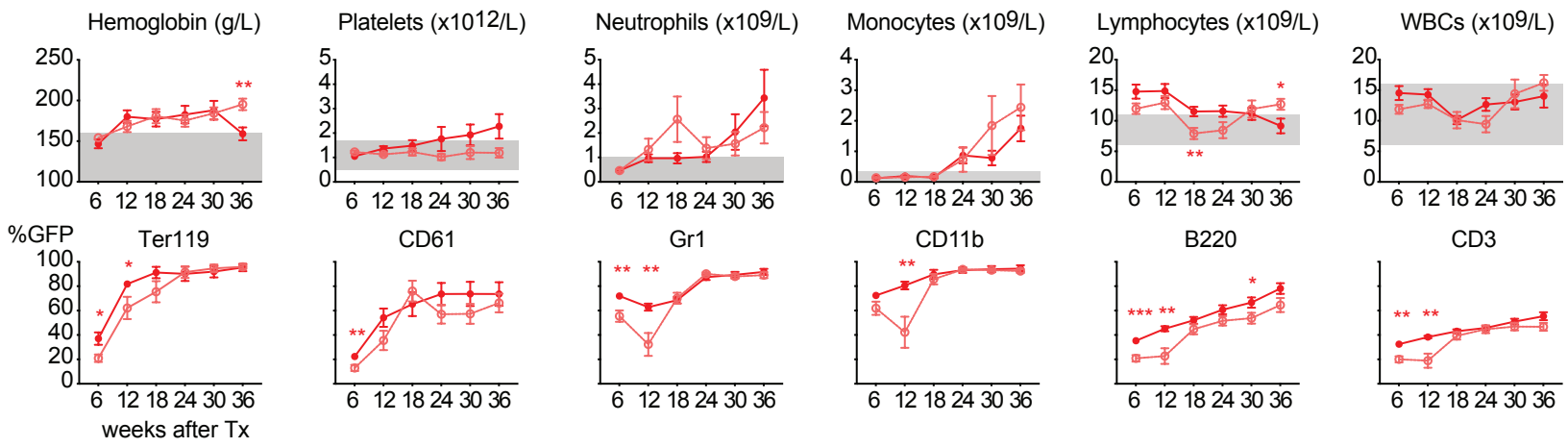

C GFP-Chimerism in HSPCs of mice that developed MPN phenotype at 36w

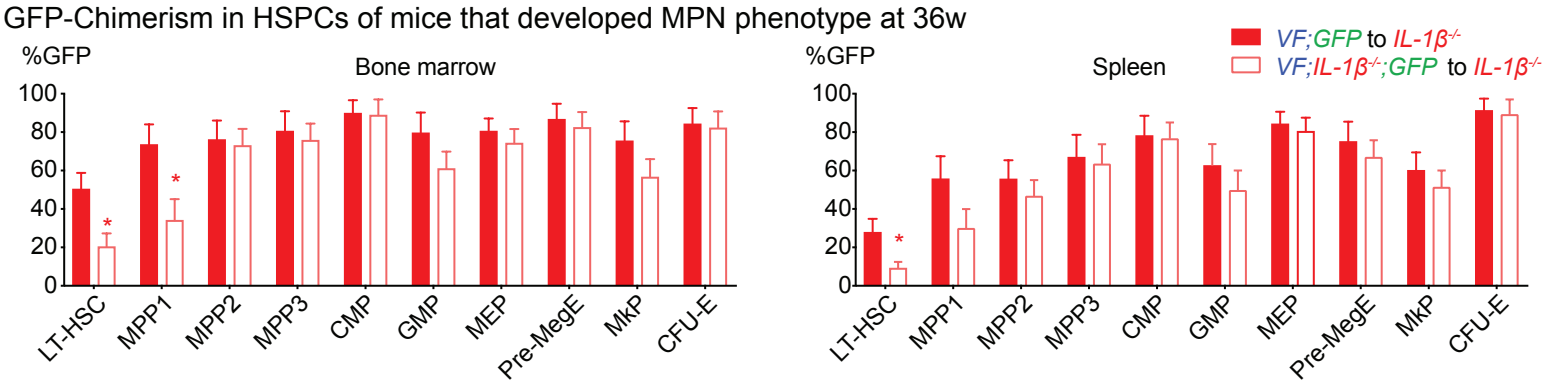

D Reticulin fibrosis in mice that developed MPN phenotype at 36w

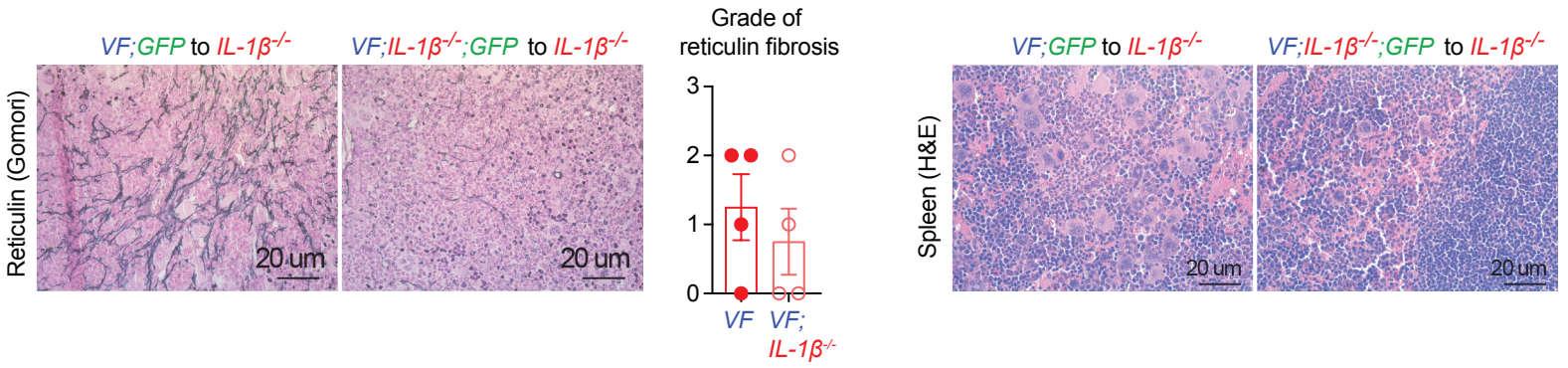

E Inflammatory cytokines in mice that developed MPN phenotype at 36 weeks

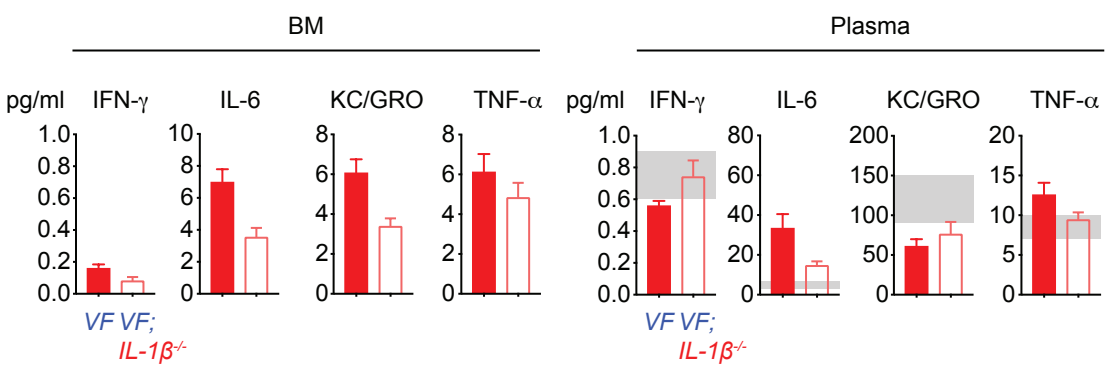

F IL-1α and IL-1Ra in BM at 36 weeks

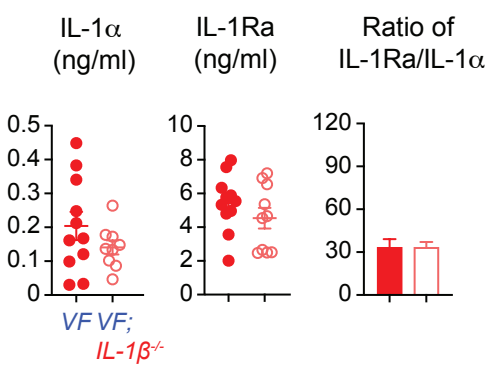

Legend to Supplemental Figure 2 (related to Figure 1)

Supplementary Figure 2. Loss of *IL-1β* from *JAK2*-mutant hematopoietic cells reduces MPN disease initiation (Transplantation at 1:100 dilution into *IL-1β*$^{-/-}$ recipients with *IL-1β*$^{-/-}$ competitor cells). (A) Schematic drawing of the experimental setup for competitive transplantation at 1:100 dilution into *IL-1β*$^{-/-}$ recipients. Bone marrow (BM) from *VF;GFP* or *VF;IL-1β-/-;GFP* donor mice was mixed with a 100-fold excess of BM competitor cells from *IL-1β-/-* donor. The time course of blood counts from individual mice that received BM from *VF;GFP* (upper panel) or *VF;IL-1β-/-;GFP* donors (middle panel), and the GFP chimerism in peripheral blood (lower panel) are shown. Multiple t tests were performed for statistical analyses. IL-1β protein levels in plasma and BM lavage (1 femur and 1 tibia) of mice with or without MPN phenotype is shown (right panel). Non-parametric Mann-Whitney two-tailed t test was performed for statistical comparisons. Bar graphs (bottom right) show the percentages of mice that showed engraftment defined as GFP-chimerism >1% at 18 weeks after transplantation and the percentages of mice that developed MPN phenotype (elevated hemoglobin and/or platelet counts). p values in lower panel were computed using Fisher's exact test. **(B)** Time course of mean blood counts and GFP chimerism in peripheral blood of *IL-1β*$^{-/-}$ mice transplanted with BM from *VF;GFP* or *VF;IL-1β-/-;GFP* and *IL-1β*$^{-/-}$ competitor cells that developed MPN phenotype during 36-weeks follow-up. Multiple t tests were performed for statistical analyses. **(C)** GFP-chimerism in hematopoietic stem and progenitor cells (HSPCs) at 36 weeks after transplantation in BM (left) and spleen (right) of *IL-1β*$^{-/-}$ mice transplanted with BM from *VF;GFP* or *VF;IL-1β-/-;GFP* and *IL-1β*$^{-/-}$ competitor cells that developed MPN phenotype. Multiple t tests were performed for statistical analyses. **(D)** Representative images of reticulin fibrosis staining in BM (left panel) and H&E staining in spleen (right panel) of mice showed MPN phenotype at 36 weeks after transplantation. Histological grade of reticulin fibrosis in BM is shown in a bar graph (right). **(E)** Levels of Inflammatory cytokines in BM lavage (1femur and 1 tibia) and plasma of mice that displayed MPN phenotype at 36 weeks after transplantation. **(F)** IL-1α and IL-1Ra levels (pg/ml) in BM of mice (from Supplemental Figure S2A) that showed MPN phenotype. Bar graph showing ratio of IL-1Ra to IL-1α in BM. p value was computed using unpaired two-tailed t-tests with Welch's correction. Grey shaded area represents normal range. All data are presented as mean ± SEM. *P < .05; **P < .01; ***P < .001; ****P < .0001.

Supplemental Figure 3 (related to Figure 2)

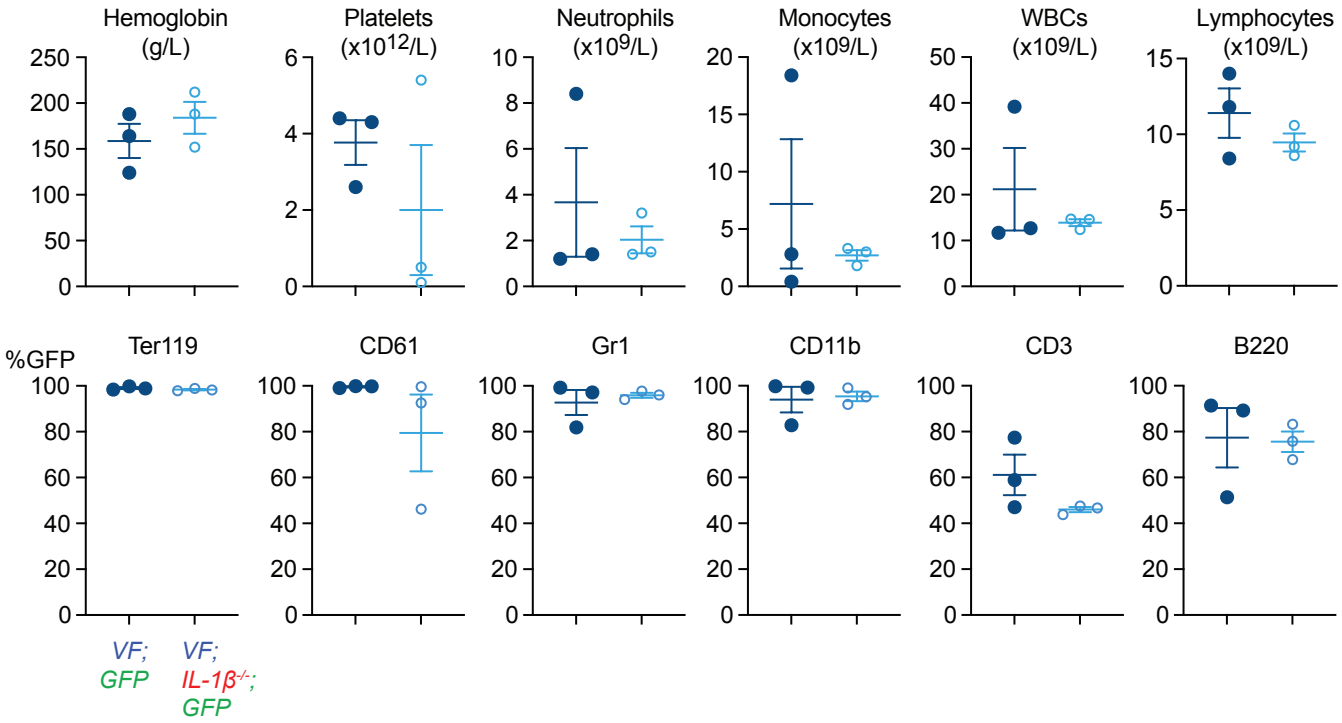

Supplemental Figure 3. Blood counts and GFP chimerism of donor mice used for secondary transplantations. Analysis was performed 36 weeks after the initial transplantation. All data are presented as mean ± SEM.

Supplemental Figure 4 (related to Figure 2)

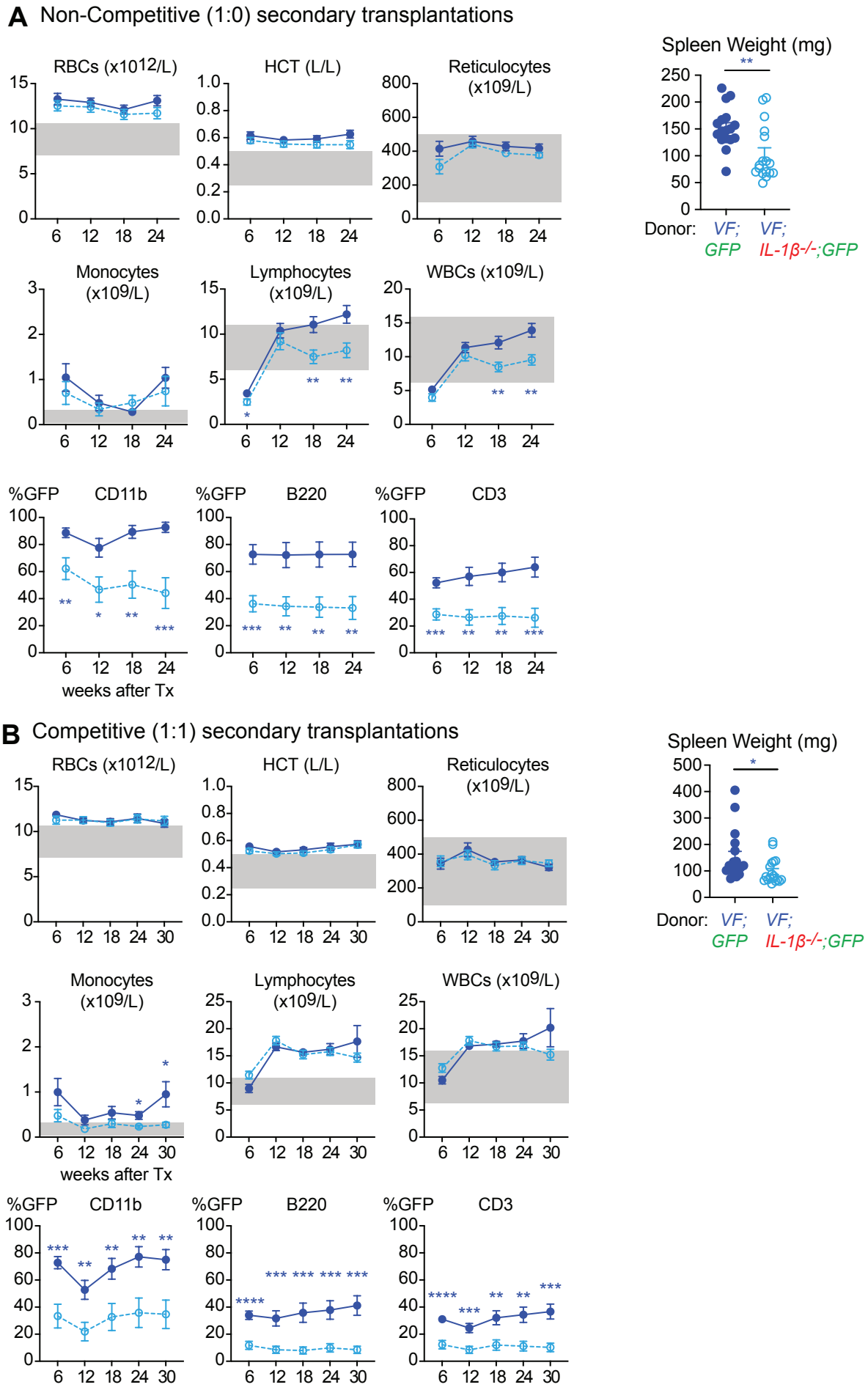

Supplemental Figure 4. (A) Red cell parameters and leukocyte counts in secondary transplanted (1:0) mice. Mean GFP-chimerism in CD11b+ monocytes, B220+ B cells and CD3+ T cell lineage is shown. Spleen weight of mice at terminal analysis is shown for both groups. **(B)** Red cell parameters and leukocyte counts in secondary transplanted (1:1) mice. Mean GFP-chimerism in CD11b+ monocytes, B220+ B cells and CD3+ T cell lineage is shown. Spleen weight of mice at terminal analysis is shown for both groups. Grey shaded area represents normal range. All data are presented as mean ± SEM. *P < .05; **P < .01; ***P < .001; ****P < .0001.

Supplemental Figure 5 (related to Figure 3A): Competitive transplantations at 1:100 dilution into wildtype (*WT*) recipients

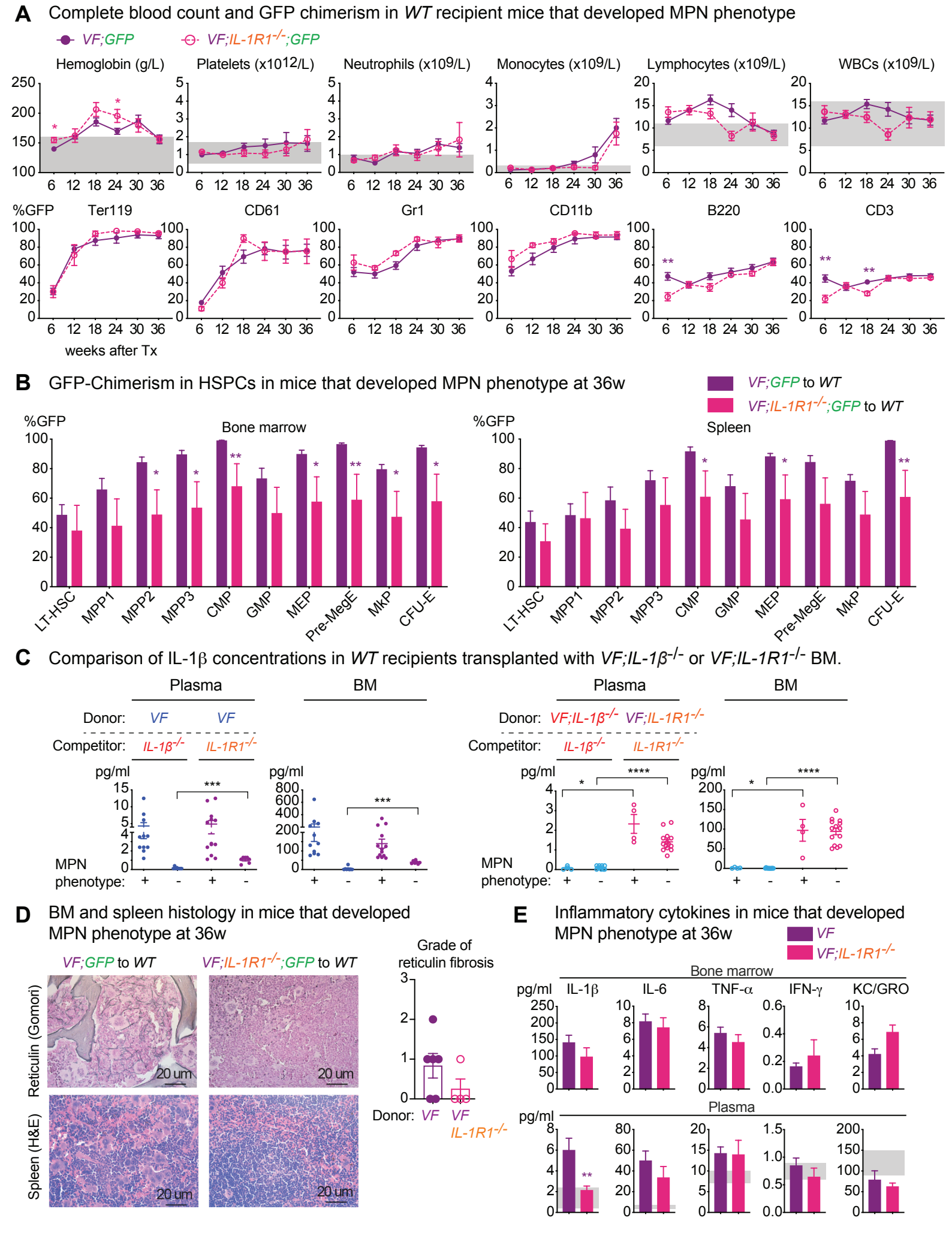

Legend to Supplemental Figure 5 (related to Figure 3A)

Supplemental Figure 5. Transplantation at 1:100 dilution into wildtype (WT) recipients with IL-1R1$^{-/-}$ competitor cells. (A) Mean blood counts and GFP chimerism in Ter119, CD61, Gr-1, CD11b (monocytes), B220 (B cells) and CD3 (T cells) in the peripheral blood of WT mice transplanted with BM from VF;GFP or VF;IL-1R1$^{-/-}$;GFP and IL-1R1$^{-/-}$ competitor cells that developed MPN phenotype during 36-weeks follow-up. Multiple t tests were performed for statistical analyses. **(B)** GFP-chimerism in HSPCs in BM (left) and spleen (right) of WT mice transplanted with BM from VF;GFP or VF;IL-1R1$^{-/-}$;GFP and IL-1R1$^{-/-}$ competitor cells that developed MPN phenotype at 36 weeks after transplantation. Multiple t tests were performed for statistical analyses. **(C)** Comparison of IL-1β concentrations in *WT* recipients transplanted with VF;IL-1β$^{-/-}$ or VF;IL-1R1$^{-/-}$ bone marrow. Data compiled from Figures 1C and 3C is presented in the same graph for easier comparison. **(D)** Representative images of reticulin fibrosis staining in BM (upper panel) and H&E staining in spleen (lower panel) of mice that developed MPN at 36 weeks after transplantation. Histological grade of reticulin fibrosis in BM is shown in a bar graph (right). **(E)** Levels of Inflammatory cytokines in BM lavage (1femur and 1 tibia) and plasma of mice that developed MPN at 36 weeks after transplantation. Grey shaded area represents normal range. All data are presented as mean ± SEM. Multiple t tests were performed for statistical analyses. *P < .05; **P < .01; ***P < .001; ****P < .0001.

Supplemental Figure 6 (related to Figure 3B): Competitive transplantations at 1:100 dilution into *IL-1R1*$^{-/-}$ recipients

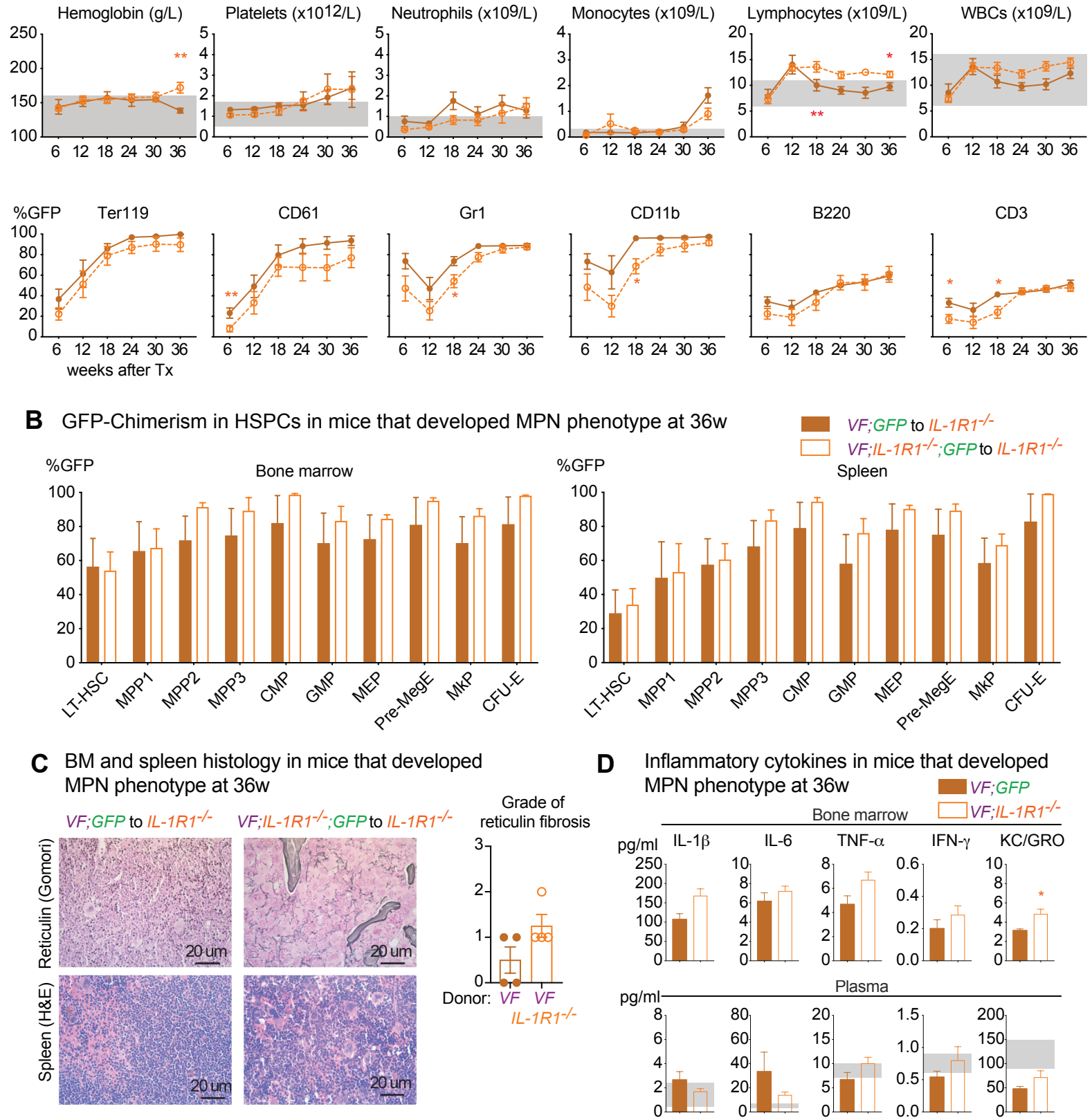

Supplemental Figure 6. Transplantation at 1:100 dilution into *IL-1R1*$^{-/-}$ recipients with *IL-1R1*$^{-/-}$ competitor cells. (A) Mean blood counts and GFP chimerism in Ter119, CD61, Gr-1, CD11b (monocytes), B220 (B cells) and CD3 (T cells) in the peripheral blood of IL-1R1$^{-/-}$ mice transplanted with BM from VF;GFP or VF;IL-1R1$^{-/-}$;GFP and IL-1R1$^{-/-}$ competitor cells that developed MPN phenotype during 36-weeks follow-up. Multiple t tests were performed for statistical analyses. **(B)** GFP-chimerism in HSPCs in BM (left) and spleen (right) of IL-1R1$^{-/-}$ mice transplanted with BM from VF;GFP or VF;IL-1R1$^{-/-}$;GFP and IL-1R1$^{-/-}$ competitor cells that developed MPN phenotype at 36 weeks after transplantation. Multiple t tests were performed for statistical analyses. **(C)** Representative images of reticulin fibrosis staining in BM (upper panel) and H&E staining in spleen (lower panel) of mice that developed MPN at 36 weeks after transplantation. Histological grade of reticulin fibrosis in BM is shown in a bar graph (right). **(D)** Levels of Inflammatory cytokines in BM lavage (1femur and 1 tibia) and plasma of mice that developed MPN at 36 weeks after transplantation. Grey shaded area represents normal range. All data are presented as mean ± SEM. Multiple t tests were performed for statistical analyses. *P < .05; **P < .01; ***P < .001; ****P < .0001.

Supplemental Figure 7

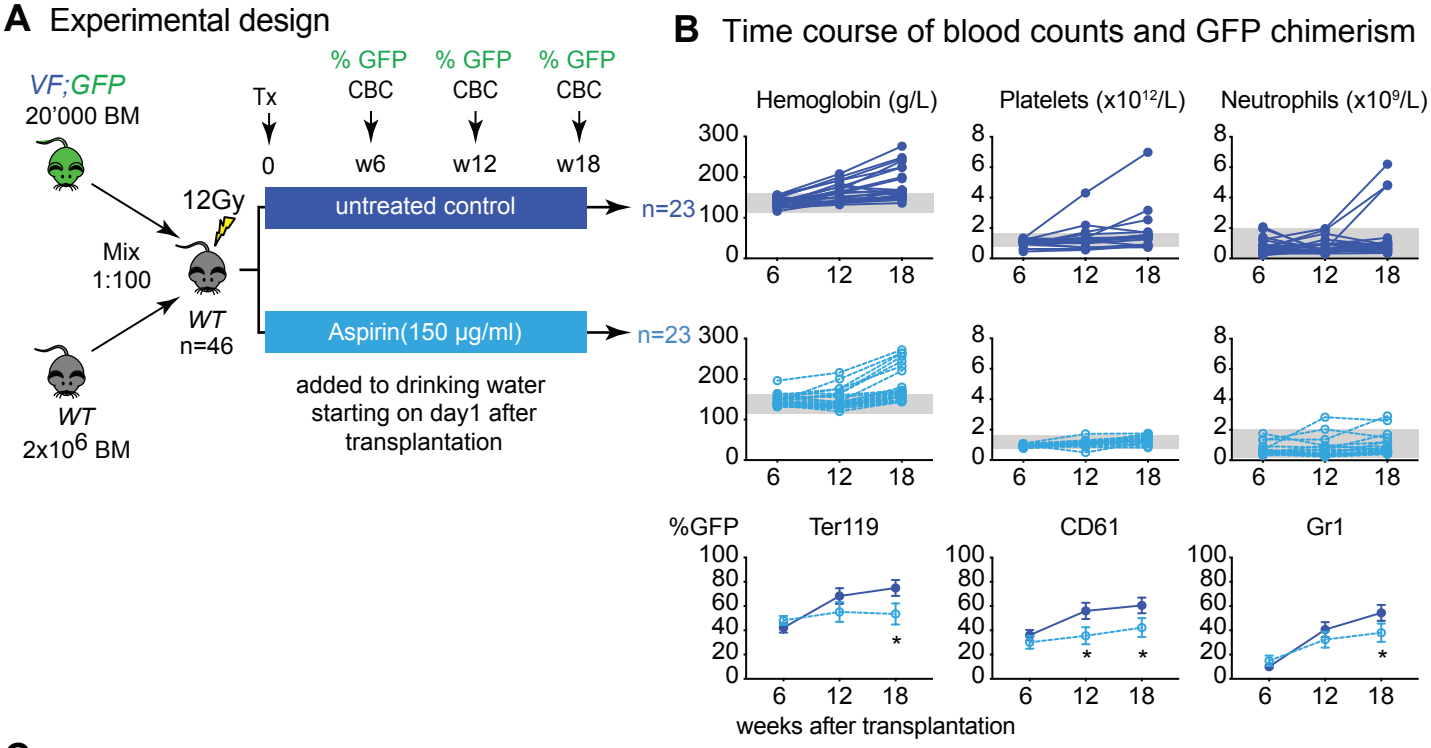

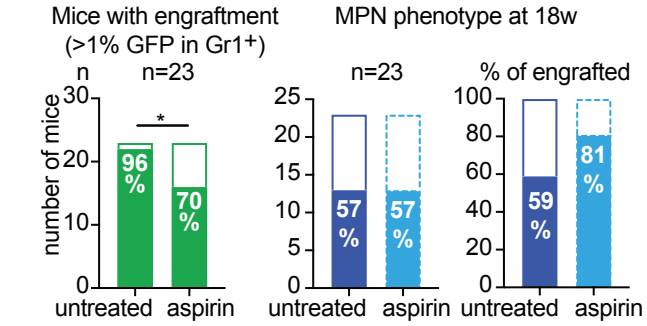

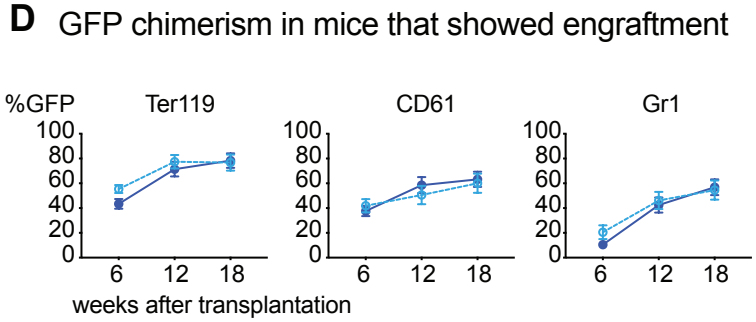

Supplemental Figure 7. Effects of Aspirin on MPN disease initiation in a mouse model of JAK2-V617F driven clonal hematopoiesis (A) Schematic drawing of the experimental setup for competitive transplantation at 1:100 dilution. Bone marrow (BM) from a *VF;GFP* donor mouse was mixed with a 100-fold excess of BM competitor cells from a *WT* donor. Mice were randomized into two treatment arms one day after transplantation and treated with either Aspirin or nothing in the driniking water (150 µg/ml) for 18 weeks. **(B)** The time course of blood counts from individual mice for the two treatment arms is shown (top and middle panel). Mean GFP (mutant cell) chimerism in peripheral blood erythroid (Ter119), megakaryocytic (CD61), granulocytic (Gr1) cells are shown in the bottom panel. Multiple t tests were performed for statistical analyses. **(C)** Bar graph showing the percentage of mice that showed engraftment defined as GFP-chimerism >1% at 18 weeks after transplantation. **(D)** Mean GFP (mutant cell) chimerism in peripheral blood of engrafted mice (engraftment defined as GFP-chimerism >1%) at 18 weeks after transplantation. p value in right panel was computed using Fisher's exact test. Grey shaded area represents normal range. All data are presented as mean ± SEM. *P < .05; **P < .01; ***P < .001; ****P < .0001.

Supplemental Figure 8 (related to Figure 4)

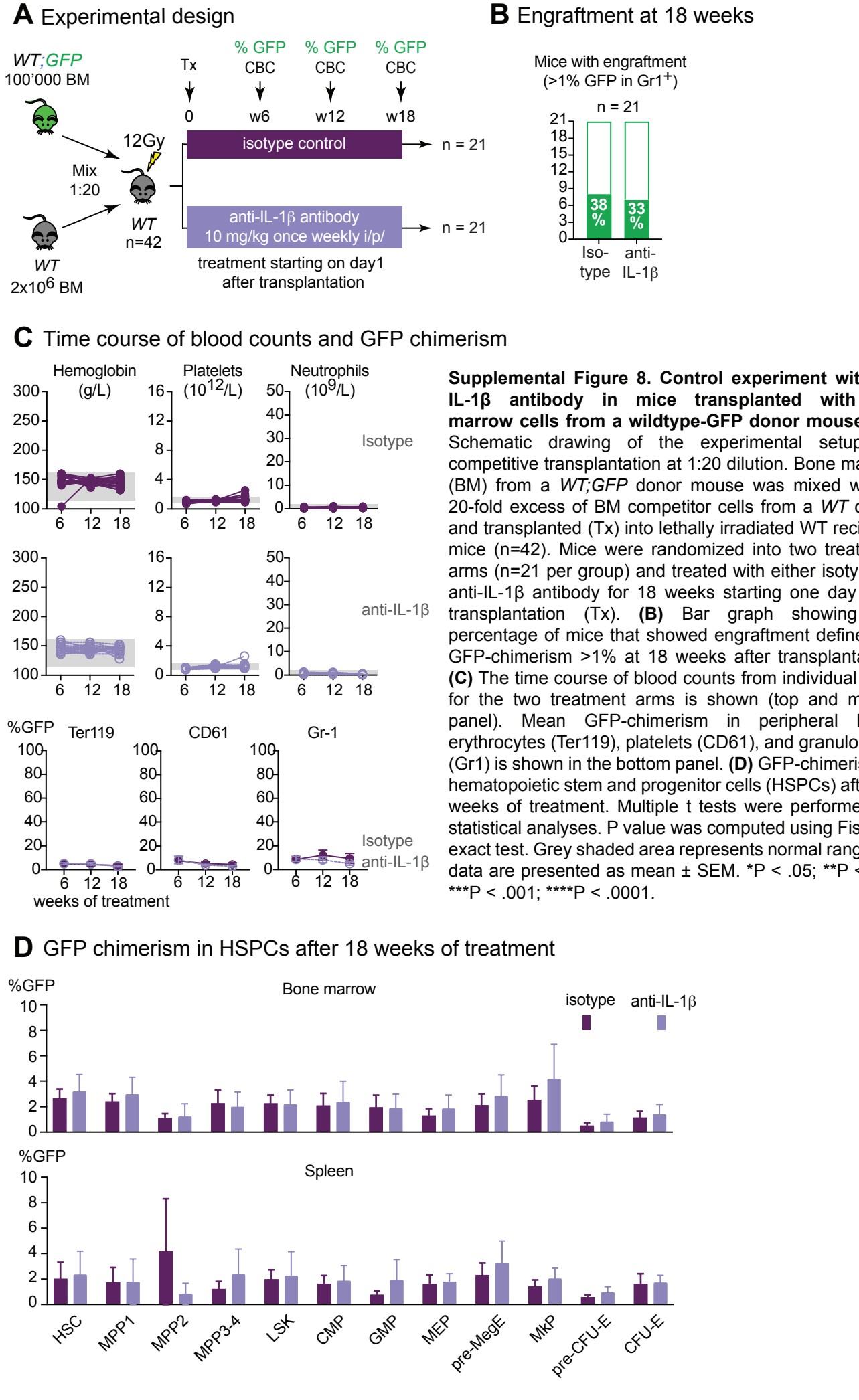

Supplemental Figure 8. Control experiment with anti-IL-1β antibody in mice transplanted with bone marrow cells from a wildtype-GFP donor mouse. (A) Schematic drawing of the experimental setup for competitive transplantation at 1:20 dilution. Bone marrow (BM) from a *WT;GFP* donor mouse was mixed with a 20-fold excess of BM competitor cells from a *WT* donor and transplanted (Tx) into lethally irradiated WT recipient mice (n=42). Mice were randomized into two treatment arms (n=21 per group) and treated with either isotype or anti-IL-1β antibody for 18 weeks starting one day after transplantation (Tx). **(B)** Bar graph showing the percentage of mice that showed engraftment defined as GFP-chimerism >1% at 18 weeks after transplantation. **(C)** The time course of blood counts from individual mice for the two treatment arms is shown (top and middle panel). Mean GFP-chimerism in peripheral blood erythrocytes (Ter119), platelets (CD61), and granulocytes (Gr1) is shown in the bottom panel. **(D)** GFP-chimerism in hematopoietic stem and progenitor cells (HSPCs) after 18 weeks of treatment. Multiple t tests were performed for statistical analyses. P value was computed using Fisher's exact test. Grey shaded area represents normal range. All data are presented as mean ± SEM. *P < .05; **P < .01; ***P < .001; ****P < .0001.

Supplemental Figure 9 (related to Figure 6)

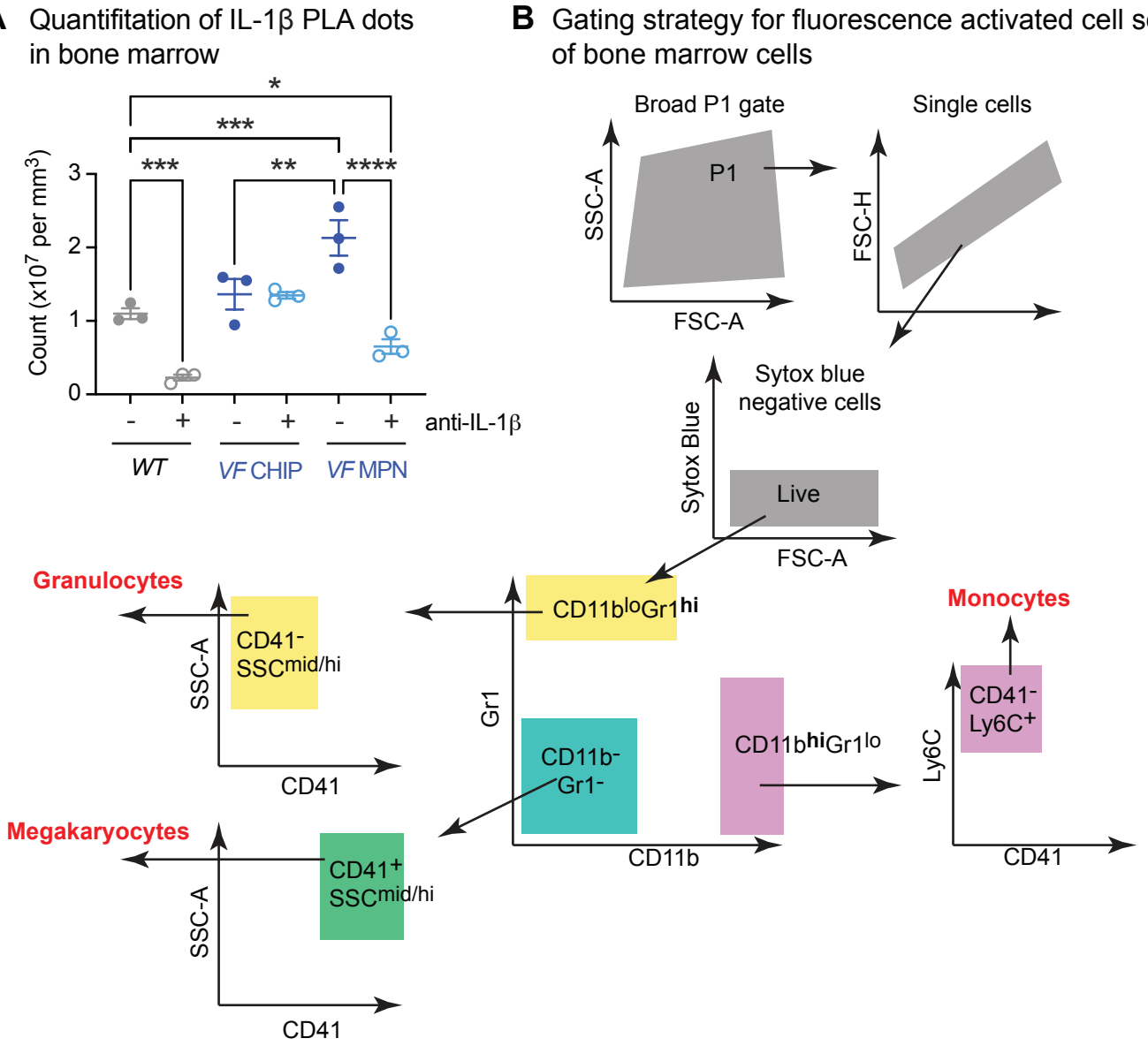

C *IL-1β* mRNA expression (TaqMan) in sorted bone marrow cell populations

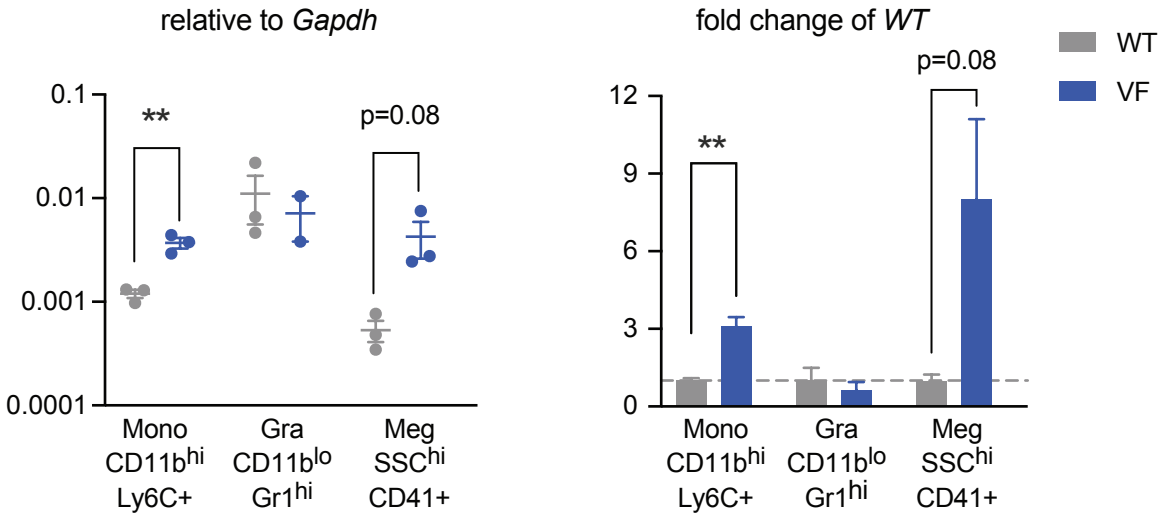

Supplemental Figure 9. **Source of IL-1β overproduction in MPN (A)** Quantification of Proximity Ligation Assay (PLA) signals in mouse bone marrow sections. **(B)** Gating strategy for FACS sorting mouse bone marrow populations **(C)** IL-1β mRNA expression in sorted bone marrow cell populations. Two-tailed unpaired t tests were performed for statistical comparisons. All data are presented as mean ± SEM. *P < .05; **P < .01; ***P < .001; ****P < .0001.

Supplemental Figure 10

A Gene-ontology (GO) enrichment analyses 2-weeks after tamoxifen induction

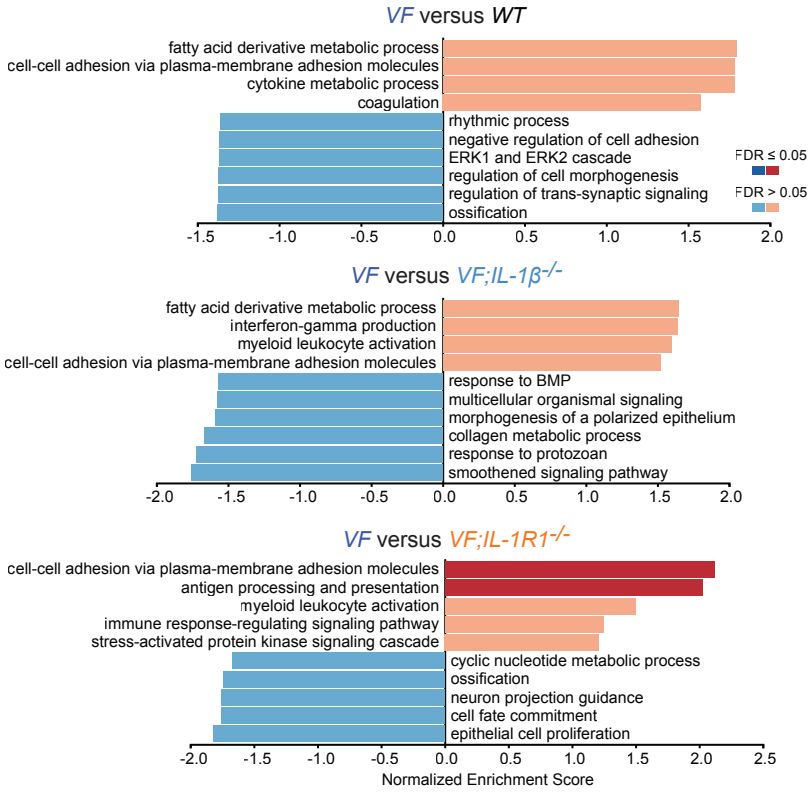

B Gene-ontology (GO) enrichment analyses 2- and 4-weeks after tamoxifen induction

VF versus WT

2-weeks after tamoxifen

Gene Set	Description	Size	Leading Edge Number	ES	NES	P Value	↑ FDR
GO:0042107	cytokine metabolic process	78	17	0.53615	1.7810	<2.2e-16	0.12156
GO:0098742	cell-cell adhesion via plasma-membrane adhesion molecules	128	29	0.49800	1.7840	<2.2e-16	0.15509
GO:1901568	fatty acid derivative metabolic process	75	17	0.54584	1.7966	<2.2e-16	0.20019
GO:0050817	coagulation	121	30	0.44986	1.5780	0.0027778	0.23978
GO:0048511	rhythmic process	197	42	-0.38733	-1.3608	0.023392	0.35250
GO:0007162	negative regulation of cell adhesion	194	44	-0.38716	-1.3642	0.023988	0.35377
GO:0001503	ossification	248	59	-0.38395	-1.3777	0.021645	0.35471
GO:0099177	regulation of trans-synaptic signaling	301	75	-0.37162	-1.3752	0.0094980	0.35622
GO:0070371	ERK1 and ERK2 cascade	221	55	-0.38587	-1.3686	0.011561	0.35707
GO:0022604	regulation of cell morphogenesis	384	85	-0.36732	-1.3698	0.0040650	0.35927

4-weeks after tamoxifen

Gene Set	Description	Size	Leading Edge Number	ES	NES	P Value	↑ FDR
GO:0035456	response to interferon-beta	48	19	0.66087	2.1549	<2.2e-16	0.0022358
GO:0010257	NADH dehydrogenase complex assembly	41	30	0.62885	1.9874	<2.2e-16	0.011924
GO:0050817	coagulation	121	29	0.51153	1.9997	<2.2e-16	0.017389
GO:0014812	muscle cell migration	74	24	-0.58848	-1.8631	<2.2e-16	0.023153
GO:0019221	cytokine-mediated signaling pathway	265	53	0.42785	1.8596	<2.2e-16	0.028320
GO:0042742	defense response to bacterium	110	22	0.48660	1.8632	<2.2e-16	0.030705
GO:0006260	DNA replication	214	120	0.43991	1.8295	<2.2e-16	0.036021
GO:0034341	response to interferon-gamma	98	30	0.49549	1.8664	<2.2e-16	0.037263
GO:0007264	small GTPase mediated signal transduction	392	130	-0.43025	-1.6028	<2.2e-16	0.094637
GO:0061564	axon development	306	94	-0.43798	-1.6052	<2.2e-16	0.095793

VF versus VF;IL-1β-/-

Gene Set	Description	Size	Leading Edge Number	ES	NES	P Value	↑ FDR
GO:0001562	response to protozoan	25	11	-0.68000	-1.7252	<2.2e-16	0.32868
GO:0007224	smoothened signaling pathway	102	25	-0.54378	-1.7555	<2.2e-16	0.33171
GO:0001738	morphogenesis of a polarized epithelium	54	21	-0.53686	-1.5886	0.0071301	0.34127
GO:0071772	response to BMP	94	28	-0.48687	-1.5704	0.011111	0.35094
GO:0035637	multicellular organismal signaling	62	20	-0.51964	-1.5770	0.0053667	0.35512
GO:0032963	collagen metabolic process	66	23	-0.54320	-1.6663	0.0035971	0.37215
GO:0002274	myeloid leukocyte activation	141	26	0.44215	1.5951	0.0026247	0.38477
GO:0032609	interferon-gamma production	79	27	0.48654	1.6392	0.0025000	0.38874
GO:0098742	cell-cell adhesion via plasma-membrane adhesion molecules	128	30	0.44109	1.5199	0.0050125	0.47071
GO:1901568	fatty acid derivative metabolic process	75	27	0.49683	1.6474	0.0024155	0.48394

Gene Set	Description	Size	Leading Edge Number	ES	NES	P Value	↑ FDR
GO:0035456	response to interferon-beta	48	27	0.71920	2.1456	<2.2e-16	0.00051230
GO:0034341	response to interferon-gamma	98	34	0.59471	1.9376	<2.2e-16	0.0051230
GO:0060326	cell chemotaxis	172	41	0.53108	1.8845	<2.2e-16	0.012551
GO:0050878	regulation of body fluid levels	212	55	0.47363	1.7031	<2.2e-16	0.069074
GO:0019221	cytokine-mediated signaling pathway	265	71	0.47631	1.7617	<2.2e-16	0.073770
GO:0055074	calcium ion homeostasis	291	74	0.46955	1.7309	<2.2e-16	0.074027
GO:0097722	sperm motility	51	15	0.56773	1.7041	<2.2e-16	0.074795
GO:0050803	regulation of synapse structure or activity	175	36	-0.33955	-1.3913	0.018182	0.66555
GO:0006836	neurotransmitter transport	172	34	-0.33354	-1.3571	0.025424	0.67726
GO:0050000	chromosome localization	71	22	-0.39125	-1.3930	0.029126	0.71176

VF versus VF;IL-1R1-/-

Gene Set	Description	Size	Leading Edge Number	ES	NES	P Value	↑ FDR
GO:0098742	cell-cell adhesion via plasma-membrane adhesion molecules	128	41	0.58417	2.1198	<2.2e-16	<2.2e-16
GO:0019882	antigen processing and presentation	65	31	0.62552	2.0268	<2.2e-16	0.0012755
GO:0050673	epithelial cell proliferation	268	93	-0.50200	-1.8217	<2.2e-16	0.085159
GO:0097485	neuron projection guidance	117	35	-0.53059	-1.7539	<2.2e-16	0.093250
GO:0001503	ossification	248	61	-0.47998	-1.7438	<2.2e-16	0.094276
GO:0045165	cell fate commitment	128	36	-0.51857	-1.7541	<2.2e-16	0.10798
GO:0009187	cyclic nucleotide metabolic process	24	10	-0.66303	-1.6662	0.0087566	0.11203
GO:0031098	stress-activated protein kinase signaling cascade	220	40	0.31829	1.2111	0.051282	0.71550
GO:0002274	myeloid leukocyte activation	141	36	0.40816	1.4977	0.0054795	0.72984
GO:0002764	immune response-regulating signaling pathway	231	43	0.32243	1.2458	0.053968	0.74423

Gene Set	Description	Size	Leading Edge Number	ES	NES	P Value	↑ FDR
GO:0035456	response to interferon-beta	48	25	0.76445	2.3292	<2.2e-16	<2.2e-16
GO:0042742	defense response to bacterium	110	33	0.60973	2.1322	<2.2e-16	0.00025885
GO:0019221	cytokine-mediated signaling pathway	265	58	0.53402	2.0759	<2.2e-16	0.00041417
GO:0019882	antigen processing and presentation	65	35	0.59970	1.9265	<2.2e-16	0.011562
GO:0060326	cell chemotaxis	172	36	0.49831	1.8419	<2.2e-16	0.025195
GO:0006260	DNA replication	214	84	-0.46498	-1.9757	<2.2e-16	0.031451
GO:0007059	chromosome segregation	275	86	-0.42707	-1.8658	<2.2e-16	0.057043
GO:0000910	cytokinesis	123	38	-0.45529	-1.8155	<2.2e-16	0.060127
GO:1904029	regulation of cyclin-dependent protein kinase activity	67	19	-0.48066	-1.7101	<2.2e-16	0.095175
GO:0071824	protein-DNA complex subunit organization	144	60	-0.41263	-1.6895	<2.2e-16	0.095362

Supplemental Figure 10. (A) Pathway analysis 2 weeks after tamoxifen induction performed with WebGe-stalt online tool (ref. (32)), using geneontology as the functional database. Minimum and maximum number of genes for a category was set to 15 and 500 respectively. TOP method was used to identify significance levels of the enriched catego-ries and number of permutations was 1000. Bars representing significant pathways (FDR<0.05) are colored according to their Normalized Enrichment Score and the false discovery rate (FDR) as indicated. **(B)** List showing enriched GO terms, number of leading edges (number of genes from each GO term matching with the genes from RNAseq dataset), FDR values and p values from the pathway analyses performed 2- and 4-weeks after tamoxifen induction.

Supplemental Figure 11

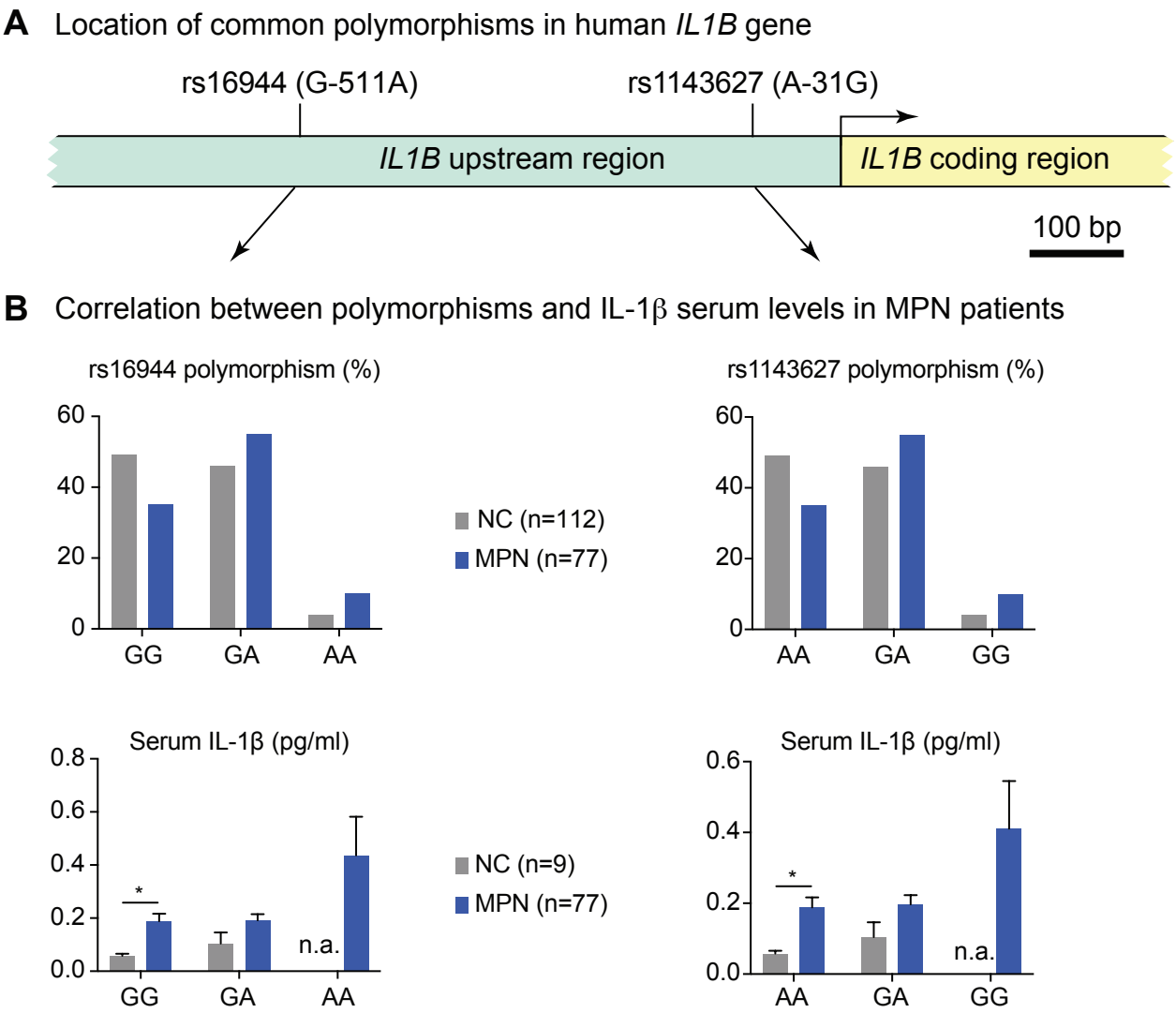

Supplemental Figure 11. *IL1B* polymorphisms are associated with increased serum IL-1β levels in MPN patients. **(A)** Location of two most commonly studied IL1B SNPs in the IL1B gene. **(B)** Bar graph showing the frequency of geno-types for IL1B SNP rs16944 (-511G/A) and serum IL-1β levels of individuals with different genotypes in normal controls (NC) and MPN patients (left panel). Bar graph showing the frequency of genotypes for IL1B SNP rs1143627 (-511G/A) and serum IL-1β levels of individuals with different genotypes in normal controls (NC) and MPN patients (right panel). Two-tailed unpaired t tests were performed for statistical com-parisons. All data are presented as mean ± SEM. *P < .05; **P < .01; ***P < .001; ****P < .0001.

Supplemental methods

Patients and healthy controls

Blood samples and clinical data of MPN patients were collected at the University Hospital Basel, Switzerland. Blood samples from healthy controls were obtained from the local blood donation center (Stiftung Blutspendezentrum SRK beider Basel). The study was approved by the local Ethics Committees (Ethik Kommission Beider Basel). Written informed consent was obtained from all patients in accordance with the Declaration of Helsinki. The diagnosis of MPN was established according to the World Health Organization and International Consensus Classification criteria (45, 46). Information on diagnosis and gene mutations of MPN patients included in this study are specified in Supplemental Table 1.

Flow cytometry and fluorescence activated cell sorting

BM cells were harvested from long bones (2 tibias and 2 femurs) by crushing bones in staining media (Dulbecco's PBS+ 3% FCS+ pen/strep). Cells were filtered through 70μm nylon mesh to obtain a single-cell suspension. Total spleen cells were harvested by crushing the spleen against 100 μm cell strainer. Red blood cells were lysed (ACK buffer, Invitrogen) and stained with following antibodies for FACS analysis: A mixture of biotinylated monoclonal antibodies CD4, CD8, B220, TER-119, CD11b, and Gr-1 was used as the lineage mix (Lin) together with Sca-1-APC-Cy7, c-kit-BV711, CD48-AF700, CD150-PE-Cy7, CD16-PE, CD41-BV605, CD105-PerCP-Cy5.5 all from BioLegend and CD34-AF647 (BD biosciences) were used as primary antibodies. Cells were washed and stained with streptavidin pacific blue secondary antibody (Invitrogen). Mouse stromal cells were obtained by crushing mouse bones directly in 0.25% collagenase I in 20% FBS/PBS solution and digesting bones and cells at 37ºC water bath for 45 minutes. Cells were filtered through 70μm nylon mesh, red blood cells were lysed (ACK buffer, Invitrogen) and cells were stained with CD45-PE-Cy7, CD31-PerCP-Cy5.5,

TER-119-APC, Sca-1-APC-Cy7, PDGFRα-PE from BioLegend. Sytox-Blue or Green (Invitrogen) was used to exclude dead cells during FACS analysis. Live, singlet cells were selected for gating. Cells were analyzed on a Fortessa Flow Cytometer (BD biosciences). Data were analyzed using FlowJo (version 10.7.1) software. Mouse BM populations including monocytes, granulocytes and megakaryocytes were FACS sorted directly in PicoPure RNA extraction buffer (Applied Biosystems). Sorting and gating strategy is described in Supplemental Figure S9.

RNA isolation and qPCR

RNA from FACS sorted monocytes, megakaryocytes and granulocytes from bone marrow of *WT* and *VF* mice were prepared using PicoPure RNA isolation kit (Applied Biosystems). RNA was then reverse transcribed to cDNA using High-Capacity cDNA Reverse Transcription Kit from Applied Biosystems according to manufacturer's instructions. *IL-1β* and *Gapdh* gene expression in mouse bone marrow populations were quantified by TaqMan gene expression assay (Assay ID: and; ThermoFisher Scientific). Each sample was run in triplicates using 2-5 ng cDNA in a 384 well plate and the qPCR was performed using VIIA 7 real time PCR instrument from Applied Biosystems.

Cytokine analysis

Mouse blood was drawn by cardiac puncture and collected in ETDA tubes. Platelet depleted plasma was collected by centrifuging the blood at 5000g for 20 minutes at 4ºC. Mouse BM lavage was prepared by flushing one femur and one tibia with 500µl ice-cold PBS and centrifuging the cell suspension at 300g for 10 minutes at 4ºC. IL-1β and other pro-inflammatory cytokine levels in mouse BM and plasma were measured by ELISA kits from R&D systems and Mesoscale Discovery according to manufacturer's instructions. Single analyte data was plotted in GraphPad

Prism software using an XY data table and the standard curve was analyzed using a sigmoidal 4-PL equation and the values of unknowns were interpolated. Multiplex cytokine data from a 96-well plate was read using Mesoscale Meso Sector S 600 instrument and the data was analyzed with Discovery Workbench 4.0 software.

Histology

Bones (sternum and/or femur), spleens and livers were fixed in paraformaldehyde, embedded in paraffin and tissue sections were stained with H&E, or Gömöri. Pictures were taken with 10x, 20x and 40x objective lens using Nikon Ti inverted microscope and NIS Software. All histological assessments of BM, spleen and liver were performed by an experienced hemato-pathologist who had no information about the genotypes or the treatment modalities. For staining of nerve fibers and Schwann cells, mouse skull bones were fixed in 2% formaldehyde/PBS solution for 2 hours at 4^{o}C, washed with PBS and stored in PBS at 4^{o}C until further analysis. Femurs were fixed on a shaker with 2% formaldehyde/PBS solution for 24 hours at 4^{o}C, then washed with PBS and decalcified with 250mM EDTA solution for 10-12 days at 4^{o}C. Decalcified bones were transferred to 30% sucrose/PBS solution for 24 hours and then to 50% OCT and 50% (30% sucrose/PBS) solution for another 24 hours. Bones were then embedded in OCT and kept at -80^{o}C until cryostat sections and the whole mount staining of the skull bones were performed. The antibodies used for immunofluorescence staining were anti-TH (Rabbit pAb, Millipore) and anti- GFAP (Rabbit pAb, Dako). Confocal images were acquired with a laser scanning confocal microscope (Zeiss LSM 700). At least 3 different sections were used for quantification using ImageJ software.

Immunofluorescence and Proximity Ligation Assay

Proximity Ligation Assay (PLA) and immunofluorescence staining of femur sections were performed as previously described.(30) Briefly, femurs were fixed in 4% methanol-free formaldehyde (Thermo Scientific) for 24 hours at 4 °C post dissection. After 14-day decalcification in 10% EDTA (BioSlove, pH 8), femurs were embedded in 4% low-gelling temperature agarose (Merck) and sectioned with a vibratome (Leica VT1200 S) into 150 µm thick sections. Staining steps were performed at room temperature (20-25°C) on superfrost glass slides (VWR) in double adhesive GeneFrame Chambers (Thermo Scientific) with gentle rocking. Sections were blocked and permeabilized with 10% donkey serum (Jackson ImmunoResearch), 1% Triton X-100 (PanReac AppliChem), 0.05% Tween-20 (Merck), 20% DMSO (Merck) in TBS (0.1M Tris, 0.15M NaCl, pH 7.5) for 2 hours minimum. Primary PLA antibodies, chicken polyclonal anti-GFP (Aves; GFP-1020), rabbit polyclonal anti-IL1-β (Invitrogen; P420B), rat IgG2b monoclonal anti-CD11b (Invitrogen; 14-0112-82), rat IgG1 monoclonal Alexa Fluor 647 anti-CD41(Biolegend; 133934) and secondary antibodies, donkey polyclonal anti-chicken IgY AF488 (Invitrogen; A78948), donkey polyclonal anti-rabbit IgG (H+L) (Merck; DUO92005-100RXN), donkey polyclonal anti-rabbit IgG (H+L) (Merck; DUO92002-100RXN), mouse monoclonal anti-rat IgG2b (Biolegend; 408207) were applied for 2 hours. In addition, 4 washing steps, 30 minutes each, were performed between incubations. Duolink *In Situ* detection reagents Orange (Merck; DUO2007-100RXN) was used for IL1-β single molecule visualization.

Confocal Microscopy, Image Visualization and Analyses

Images were acquired on a Leica TCS SP8 confocal microscopy using Leica type G immersion liquid with a 63x glycerol immersion lens (NA 1.3, FWD 0.28 mm). The scanning was performed at 400 Hz at room temperature in bidirectional mode at 1024x1024 pixel resolution.

Only HyD detectors were used for signal acquisition. Images shown were the MIP (maximum intensity projection) from Imaris 3D reconstruction. Isosurface (CD41+ megakaryocytes and CD11b+ monocytes) and spot (IL-1β PLA) were generated, and 3D distance-transformed in Imaris v9.9.1. PLA signals in the bone, blood vessels, and nucleus were masked out. Random dots were sampled 100 times with the same number as IL-1β PLA dots, resulting in an average dot count every 1μm increment from the Isosurface. The enrichment profiles towards segmented structures were created from the ratio of IL-1β PLA dot to random dot count per distance bin.

RNA sequencing

RNA from FACS sorted long-term hematopoietic stem cell (HSC; Lin−Sca1+cKit+CD48−CD150+) from bone marrow were prepared using Picopure RNA isolation kit (Applied Biosystems). The quality and concentration of total RNA was determined on Agilent 2100 Bioanalyzer. RNA was reverse transcribed and cDNA amplified with SMART-Seq v4 (Takara). Unstranded libraries were prepared with Nextera XT (Illumina) according to manufacturer's instructions. Samples were pooled to equal molarity and run on the Fragment Analyzer for quality check and used for clustering on the NovaSeq 6000 instrument (Illumina). Samples were sequenced in paired-end mode, with 51bp read length and primary data analysis was performed with the Illumina RTA version 2.1.3 and bcl2fastq v2.20.0.422. Reads were mapped to the mouse genome mm10 with STAR (version 2.7.10a) (56) with default parameters, except filtering out multimapping reads with more than 10 alignment locations (outFilterMultimapNmax=10) and filtering reads without evidence in the spliced junction table (outFilterType="BySJout"). The mm10 genome reference was supplemented to include the construct Homo_sapiens_JAK2_V617F construct, CreERT2 and pEGFP sequences. All subsequent analyses were performed using the R software (version 4.2.2) and Bioconductor

3.16 packages. The *featureCounts* function from the Bioconductor Rsubread package (version 2.0.1) (57) was used to count the number of reads (5' ends) overlapping with the exons of each gene (Ensembl release 102 genes, CreERT2, pEGFP, and for the Homo_sapiens_JAK2_V617F construct, the CDS exons 3 to 12 and exons 13 to 25 separately) assuming an exon union model (58-60). Because RNAseq libraries were unstranded we only retained protein-coding genes for further analyses. The Bioconductor package edgeR (version 3.40.2) (61) was used for differential gene expression analysis. Samples were log2 transformed and normalized using the TMM method (61). Genes with CPM values above 1 in at least 2 samples were retained for the differential expression analysis. To test for gene expression differences between conditions, we used the quasi-likelihood testing framework (edgeR functions *glmQLFit* and *glmQLFTest*) (62). P-values were adjusted by controlling the false discovery rate (FDR; Benjamini-Hochberg method) and genes with a FDR lower than 5% were considered significant. Pathway analyses were performed using WebGestalt online tool (32), using only the differentially expressed genes between the groups of interest and using the Geneontology as the functional database. We used the TOP method of WebGestalt to determine the significance levels of the enriched categories and weighted set cover tool as a redundancy reduction method. Benjamini-Hochberg method was used for determining FDR corrected p-values for the enriched categories and pathways with FDR<0.05 were defined as significant. The minimum and maximum number of genes for a gene set category was set to 15 and 500 respectively.

Statistical analyses

The unpaired two-tailed Student's t-test analysis was used to compare the mean of two groups. Normality tests were performed to test whether the data follows a normal distribution. When the distribution was not normal, non-parametric Mann-Whitney t-tests were performed. For samples with large variances, Welch's correction was applied for t-test. Multiple t-tests with or without correction or one-way or two-way ANOVA analyses followed by Dunn's or Tukey's comparison tests for multiple group comparisons followed by Bonferroni's correction of p-

values. Data were analyzed and plotted using Prism software version 7.0 (GraphPad Inc.). All data are represented as mean ± SEM. Significance is denoted with asterisks (*$p<0.05$, **$p<0.01$, ***$p < 0.001$, ****$p < 0.0001$).

Supplemental Table 1. Characteristics of the MPN patients

UPN	Diagnosis	*Jak2*-V617F % VAF	Sex	Additional gene mutations (only if likely pathogenic)
P346A	PV	79	female	None
P354A	PV	66	female	None
P355A	PV	32	female	None
P357A	PV	43	male	None
P361A	PV	9	female	None
P362A	PV	9	female	None
P382A	PV	41	male	None
P389A	PV	49	female	None
P422A	PV	20	male	DNMT3A Pro904Leu 18%
P427A	PV	44	female	None
P443B	PV	15	male	None
P483C	PV	76	female	None
P486B	PV	52	male	NFE2 Glu297_Arg300del 15%
P489A	PV	8	male	None
P490B	PV	38	male	TERT Ala801Thr 25%
P497A	PV	80	male	None
P498A	PV	63	male	None
P500A	PV	70	female	None
P506A	PV	100	male	None
P508B	PV	83	male	None
P520A	PV	83	female	None
P529A	PV	36	male	ASXL1 Val515fs* 37%; TET2 Asn170fs* 8%
P532A	PV	45	male	None
P545A	PV	31	male	Not studied
P559A	PV	51	male	Not studied
P288A	ET	31	female	None
P317A	ET	7	female	None
P356A	ET	19	male	None
P365A	ET	25	female	None
P368A	ET	2	female	None
P369A	ET	8	female	None
P379A	ET	25	male	None
P414A	ET	35	female	None
P423A	ET	7	female	None
P432A	ET	1	female	None
P433A	ET	13	female	None
P437A	ET	29	male	None
P442A	ET	9	male	None
P460A	ET	17	male	None
P485A	ET	16	female	None
P501A	ET	3	female	None
P507A	ET	100	male	TET2 Ser585X 46%; TET2 Phe785fs* 46%
P510A	ET	28	female	None
P536A	ET	9	male	Not studied
P537A	ET	15	female	Not studied
P544A	ET	33	male	Not studied
P560A	ET	3	male	Not studied
P203A	PMF	87	male	None
P212A	PMF	47	male	None
P220A	PMF	37	male	ASXL1 Gly646Trpfs* 30%
P253A	PMF	51	male	CBL Lys382Arg 34%; SF3B1 Lys666Arg 19%
P300A	PMF	40	male	None
P316A	PMF	10	male	None
P322A	PMF	45	male	None
P350A	PMF	47	female	ASXL1 Arg965X 53%
P351A	PMF	5	female	None
P360A	PMF	22	male	CRIM1 Asn406Ser 39%; HIF3A Asp558Asn 65%
P370A	PMF	35	male	None
P373A	PMF	43	female	None
P376A	PMF	51	male	ASXL1 Asp1004fs* 41%; IDH2 Arg140Gln 43%; U2AF1 Ser34Ala 36%
P415C	PMF	73	male	None
P425A	PMF	45	male	JARID2 Ser949fs* 44%
P448A	PMF	88	female	None
P455A	PMF	57	male	ASXL1 Pro1324fs* 37%
P464A	PMF	12	male	None
P484A	PMF	96	male	None
P488A	PMF	47	male	None
P492A	PMF	14	female	None
P525A	PMF	45	male	TP53 Arg337Leu 47%; TP53 Val143Met 48%
P534A	PMF	34	female	MPL Tyr591Asp 24%
P548A	PMF	59	female	Not studied
P550A	PMF	47	female	Not studied
P561A	PMF	46	female	Not studied
P523A	Prefibrotic PMF	23	male	None
P527A	Post-ET MF	80	male	None
P531A	post PV-MF	78	male	None
P526B	post PV-MF	79	female	None